Electrochemical analysis of the first Polish coins using the voltammetry of immobilized particles

Antonio Doménech-Carbó*[a], Julio M. del Hoyo Meléndez*[b], María Teresa Doménech-Carbó[c], Joan Piquero-Cilla[a]

[a] Departament de Química Analítica. Universitat de València. Dr. Moliner, 50, 46100 Burjassot (València) Spain.
[b] Laboratory of Analysis and Non-Destructive Investigation of Heritage Objects, National Museum in Krakow, Krakow 31109, Poland
[c] Institut de Restauració del Patrimoni, Universitat Politècnica de València, Camí de Vera 14, 46022, València.

* Corresponding authors, E-mail: antonio.domenech@uv.es; jdelhoyo@muzeum.krakow.pl.

Keywords: Voltammetry of immobilized particles; Silver; Copper; Mediaeval Poland numismatic collections; Long-term corrosion modeling.

Abstract

A series of 20 denarii from Boleslaus the Brave (992–1025) and Mieszko II Lambert (1025–1034), corresponding to the beginning of the Polish state were studied using the voltammetry of immobilized particles (VIMP) methodology. VIMP experiments, applied to nanosamples of the corrosion layers of the coins in contact with aqueous acetate buffer, provided well-defined responses mainly corresponding to the corrosion products of copper and lead. Such voltammetric responses, combined with X-ray fluorescence (XRF) spectroscopy experiments performed on the same set of coins, and complemented by focusing ion beam-field emission scanning electron microscope (FIB-FESEM) on silver coins from the 19th century, supported the hypothesis that two different metal sources were used in former historical period and suggested that the coins were produced in three different mints.

1. Introduction

Numismatic research represents an important contribution to historic and archaeometric studies [1]. One of the cases where ancient coins possess not only a considerable archaeometric value but also a high symbolic and historic value is that constituted by those of the reigns of Mieszko I, his son Boleslaus the Brave (Bolesław Chrobry), and his grandson Mieszko II Lambert during the 10^{th}-11^{th} centuries. It is widely accepted that King Boleslaus the Brave (992–1025) created the first Polish state through the unification of Polish tribes and established the first monetary system. Remarkably, first reference to Poland in a historical source, the inscription POLONIE, appears in the PRINCES POLONIE denarius, minted by Boleslaus the Brave [2].

Boleslaus the Brave pennies, however, create some archaeometric problems. Such coins were probably coined from circa 995, and were based on the Charlemagne's monetary system established in Western Europe around the 9^{th} century. The Boleslaus the Brave pennies are represented by approximately 20 types, some of which are imitations of coins from other countries. It is believed, although there is no absolute confirmation, that Mieszko I minted his own coins, in a mint located in Greater Poland, Kuiavia or northern Masovia, and that he coined the first Polish denarius, characterized by the MISICO inscription, around 980 [3]. An alternative hypothesis was proposed by Suchodolski [4], who considered the appearance of coins during the reign of Mieszko I less probable and proposed that coins with the MISICO inscription were more likely minted by Boleslaus' son, Mieszko II Lambert during his reign in 1025–1034.

A previous study of a set of 71 silver coins using micro XRF spectrometry [5], extending a prior work on 11 coins [6], suggested that the Boleslaus coins were struck from materials that came in from two different sources and that the metallurgical procedures were improved during his reign and that of his son. Conceivably, a part of the Ag used for minting early Polish coins could have come from the melting of Arabic coins or coins minted by Muslim rulers of Central Asia [7,8], whereas another portion would be production of mines around the Baltic region [9,10].

These archaeometric matters deal with the general problems of determination of the provenance, mint and age of coins. These analytical targets have been faced using

microstructural (metallographic) analysis [1,11], neutron diffraction [12] and neutron absorption [13], isotope analysis [14,15], XRF spectrometry [15-21] and electron microscopy [22,23], among others [18]. Such techniques provide important analytical capabilities but also have limitations, as discussed for isotope analysis [14,24] and XRF [25], so that multi-technique approaches are usually recommended [26,27].

In this context, the scope of available techniques has been enhanced by the incorporation of the voltammetry of immobilized particles (VIMP). This is a solid state electrochemistry methodology, developed by Scholz et al. [28,29], whose application to a variety of materials into the archaeometric domain has been reviewed [30,31]. The VIMP has been applied to the study of metal archaeological objects [32,33] as well as their corrosion products [34-38]. The 'one-touch' sampling methodology [39], based on the use of graphite pencils [40,41], permitted the application of VIMP to authentication [42], tracing [43] and dating of archaeological lead [44] and copper/bronze [45] using sample amounts at the nanogram level. Recently, the VIMP of silver and silver-copper alloys has been studied by Capelho et al. [46] and Cepriá et al. [47]. In particular, the possibility of discriminating between different mints was previously assessed for a set of silver *croats* from four mediaeval Valencian reigns in the 13^{th}-14^{th} centuries [48]. It is pertinent to note that the VIMP technique differs from conventional solution phase voltammetry in which there is no need of dissolving the sample to place the analytes in solution. Then, VIMP provides direct information on the chemical and mineralogical composition of the sample via the solid-sate electrochemistry of the components of the sample.

Here, we report the application of VIMP to study a set of 20 coins from Boleslaus the Brave and Mieszko II devoted to gain information on their provenance and minting techniques. The crossing of VIMP with XRF data suggested that there was silver from two different provenances and that three different mints were used. The basic idea is that subtle differences in the composition and minting of the coins are reflected in the voltammetric response of the patina. To assess this approach, complementary experiments were performed on various silver coins from a private numismatic collection of 19^{th} century items using focusing ion beam-field emission scanning electron microscope (FIB-FESEM).

2. Experimental

2.1. Reference materials and samples

Reference materials (STD1 to STD6) consisted of Ag/Cu/Pb alloys that were purchased from Kruel (Chrzanów, Poland). Their chemical composition is described in Table 1. To perform FIB-FESEM experiments, two silver coins of the private collection Doménech-Francés (Spain) were used; these were one franc, Henri V King of France, France, 1831 (DF01), and one peseta, Gobierno provisional, Spain, 1869 (DF02).

Nanosamples from 20 coins of the previously studied set of 71 Polish denarii [5] were taken using the non-destructive 'one-touch' sampling protocol [39] (*vide infra*). It is pertinent to remark that sampling was carried out at the Laboratory of Analysis of the National Museum in Krakow (Poland) and the sample-modified graphite bars were later transported to Valencia (Spain) where the voltammetric measurements were performed. A detailed description of the coins was previously reported [5] and is summarized in Table 2 conjointly with the elemental composition of major elements (Ag, Cu and Pb) determined from XRF data. In this study, they were grouped on the basis of archaeological and XRF data in four groups, termed, in the following as Boleslaus 995-1005, Boleslaus 1000-1010, Boleslaus after 1010 and Mieszko 1010-1020.

2.2. VIMP measurements

Air-saturated aqueous 0.25 M sodium acetate buffer (Panreac) at pH 4.75 was used as a supporting electrolyte for electrochemical measurements and was renewed after each electrochemical run to avoid contamination due to metal ions eventually released to the solution phase during electrochemical turnovers. To test the possibility of using portable equipment, no deaeration was performed. Square wave voltammograms (SWVs), and cyclic voltammograms (CVs) were obtained on commercial paraffin-impregnated graphite bars (Staedtler S200, HB type, 2.0 mm diameter) where the sample was adhered using the 'one touch' VIMP protocols [39].

VIMP for reference materials was carried out using conventional VIMP protocols by powdering an amount of 1-2 mg of the solid in an agate mortar and pestle, and extending it on the agate mortar forming a spot of finely distributed material. Then the lower end of the graphite electrode was gently rubbed over that spot of sample and

finally rinsed with water to remove ill-adhered particles. Sample-modified graphite bars were then dipped into the electrochemical cell so that only the lower end of the electrode was in contact with the electrolyte solution. Electrochemical experiments were performed at 298 K in a three-electrode cell using a CH I660C device (Cambria Scientific, Llwynhendy, Llanelli UK). A platinum wire counterelectrode and an Ag/AgCl (3 M NaCl) reference electrode completed the three-electrode arrangement.

2.3. Micro-XRF measurements

Micro-XRF analysis was performed using a Bruker (Karlsruhe, Germany) Artax 400 XRF spectrometer equipped with a Rh tube and a 0.650 mm collimator. The X–ray generator was operated at 50 kV and 0.5 mA, while the acquisition time was 300 s. This instrument has a Si drift X-ray detector with an active area of 10 mm^2. The beam was focused on the analysis spot with the help of a laser and a camera, which are attached to the spectrometer. Acquisition and evaluation of XRF spectra were carried out using Spectra 5.3 (Bruker AXS Microanalysis, Berlin, Germany). The raw spectra and the net peak areas of the elements of interest were evaluated. Four measurements, two on each side, were performed on the coins and the reported wt% compositions are the calculated average values. For determination of Ag and Cu, the net peak areas of their Kα lines were employed, while for the determination of Pb, the Lβ line was used since it showed similar intensity to the Lα line and less peak overlap.

2.4. FIB-FESEM experiments

Sectioning and imaging of the coins was performed with a FIB-FESEM Zeiss (Orsay Physics Kleindiek Oxford Instruments) model Auriga compact equipment that enabled the characterization of the microtexture and mineral phases in the superficial corrosion layer and in the metal core of the 19^{th} century coins. The operating conditions were: voltage, 30 kV and current intensity, 500μA and 20 nA in the FIB for generating the focused beam of Ga ions and a voltage of 3 kV in the FESEM.

3. Results and discussion

3.1. Voltammetric pattern

Figure 1 shows the square wave voltammograms of samples a,b) 766 and c,d) 783 attached to a graphite electrode in contact with aqueous acetate buffer at pH 4.75. For

sample 766 the voltammograms of the sample (black lines) are superimposed to the corresponding blanks recorded at unmodified graphite electrodes (red lines) whereas for sample 783 the resulting voltammograms after subtracting the corresponding background are depicted. The response was consistent with previous reports [48] and those recorded for reference materials and consisted, in negative-going potential scans (Figure 1a) of overlaying cathodic peaks at +0.05 (C_{Ag}) and –0.10 V (C_{Cu}) preceding a more prominent reduction peak at –0.55 V (C_{Pb}), which can be attributed, respectively, to the reduction of the products of corrosion of silver (mainly AgCl), copper (mainly cuprite, Cu_2O) and lead (mainly litharge, PbO), as judged by the Tafel analysis of the respective voltammetric signals [39,49]. In the region between +0.40 and 0.00 V weak additional signals often appear, being attributable to silver-centered electrochemical processes (*vide infra*). The signal for the reduction of lead corrosion products is superimposed to the background cathodic current due to the reduction of dissolved oxygen appearing at ca. –0.65 V (C_{ox}).

In the subsequent positive-going potential scan voltammograms, intense anodic peaks appear at –0.50 V (A_{Pb}), –0.05 and 0.00 V (both labeled as A_{Cu}) and +0.10 and +0.25 V (both marked as A_{Ag}). These peaks correspond to the stripping oxidation of the metal deposits previously generated at negative potentials to the respective metal ions in the solution. Such oxidative dissolution (stripping) processes often display peak splitting, a feature which can be attributed to the previous formation of different metal deposits [50-52].

The first relevant voltammetric feature is the relatively large intensity of the lead-based signals, C_{Pb} and A_{Pb}, relative to those of copper- and silver-centered processes. This feature is in agreement with the recognized tendency of copper and lead to corrode preferentially to silver and the prevailing corrosion of lead relative to copper in leaded bronze [53].

To use these voltammetric responses for grouping the coin samples it is pertinent to note that, given the characteristics of the sampling method, there is some possibility of deposition of ‘external’ materials (dust, etc.) on the corrosion layer as a result of pedological processes and/or environmental contamination, thus distorting its

electrochemical response. These effects were possibly minimally influential in our case because: i) sampling was performed on selected locations of the coins characterized by uniform corrosion layers; ii) most of the components of 'external' materials (clays, calcareous minerals) are electrochemically silent under our experimental conditions.

A more detailed examination of the voltammetric profiles permitted to establish a grouping of the samples. Thus, Figure 2 depicts the region of negative-going SWVs where the signals C_{Ag} and C_{Cu} appear for a reference material containing 96%wt Ag plus 4%wt Cu, and different coin samples. In reference materials, the cuprite reduction signal at –0.10 V is preceded by weak, but well-defined signals at +0.35 and +0.20 V which can be assigned to the reduction of silver acetate, formed by the previous electrochemical oxidation of silver at the more positive potentials at which the voltammogram was started, and AgCl, respectively [49,50]. Remarkably, a set of coin samples (labeled as a type A in the following), such as coin 800 (Fig. 2b) displayed well-defined silver acetate signals whereas another group of coin samples (type B in the following) did not present such signals and only the AgCl reduction process at ca. +0.05 V appeared showing a strong overlap with the cuprite reduction peak appeared (Figs 2c,d for coins 796 and 762, respectively). Table 3 summarizes the observed voltammetric processes.

A more complex grouping was suggested by the examination of the positive-going scan voltammograms. As can be seen in Figure 3, the region of potentials, where the stripping of copper and silver are recorded, displays clearly different profiles but grouped in few common patterns. Thus, the coins of type A displayed in general both peaks A_{Ag} and A_{Cu} with significant peak splitting, as can be seen in Figs. 3a,b for coins 793 and 795, respectively. In contrast, samples of type B displayed a unique, prominent A_{Cu} peak accompanied by isolated A_{Ag} signals (Figs. 3c,d for coins 782 and 791) or by considerably weak A_{Ag} signals, as depicted in Figs. 3e,f for coins 753 and 788.

The above differences in the cathodic and anodic patterns of coin samples can be interpreted on considering that, due to the mode of surface sampling, the voltammograms reflect not only the chemical and mineralogical composition of the corrosion layers of the coins, but also the 'textural' properties of this corrosion layer, representative of the shape and size distribution and adherence to graphite of the grains

of the compounds forming the corrosion layers of the coins. In turn, these properties can be considered as dependent on the chemical composition of the base metal, its 'corrosion history' but also of the minting procedures (*vide infra*). In the following, it will be assumed that, in agreement with physical examination of the coins, all the studied samples correspond to coins which were subjected to a similar process of corrosion so that differences can be attributed to both compositional and mint differences between them.

3.2. XRF and VIMP grouping

Figure 4a depicts the variation of the percentage of Cu on the percentage of Ag, determined from XRF data in ref. [5], for the studied coins. All data points fall in a narrow region corresponding to an apparently linear relationship between both quantities. This result suggests that there is a common compositional pattern in the base metal where increasing the copper content is accompanied by a parallel decrease in the silver content. In contrast, the representation of the percentage of Pb vs. the percentage of Ag does not provide any logical correlation. As can be seen in Figure 4b, there is a series of coin samples for which there is an apparent tendency of increasing the Pb content on increasing the Ag content. Such samples, interestingly, are those designed as forming the type A from voltammetric data. The samples of the voltammetric type B, however, were confined to a relatively narrow region in the Pb wt% vs. Ag wt% diagram and these samples show a low Pb content apparently independent on the Ag content.

The consistency of VIMP and XRF data acts in support of the hypothesis that two different metal sources were used [5]. Conceivably, samples of the type A would have been prepared from lead-containing silver with more or less copper content whereas samples of the type B would have been prepared from well-refined silver with minor amounts of lead. Previous reports confirm these advancements in cupellation processes of silver since ancient times [54,55].

The crossing of data from XRF and VIMP measurements produced an additional grouping of coin samples. For this purpose, the ratio between the peak currents of the peaks C_{Cu} and C_{Pb} in SWVs was used, as shown in Figure 1a. The ratio between the cathodic signals corresponding to the reduction of copper and lead corrosion products,

$i_p(C_{Cu})/i_p(C_{Pb})$, was found to be representative of the corrosion advance in leaded bronze statuary and ultimately representative of the age of the objects [53], providing a reasonable parameter to be similarly studied when analyzing silver coins. Figure 5a depicts the plots of $i_p(C_{Cu})/i_p(C_{Pb})$ vs. the weight percentage of Cu for coin samples considered in this study. One can see in this figure that the data points appear to be confined in three regions that define three differentiated curved paths. A similar grouping can be seen in Figure 5b, which corresponds to the variation of $i_p(C_{Cu})/i_p(C_{Pb})$ vs. the percentage of Ag.

These results suggest that there is the possibility of considering the observed grouping as a result of the confluence of two factors: differences in the base metal (types A and B) and textural differences resulting from the use of three different mints (labeled in the following from I to III).

3.3. VIMP plus FIB-FESEM experiments

In order to test the hypothesis that textural differences associated to different mints can be reflected in the voltammetric response of the corrosion layers of coins, FIB-FESEM experiments were performed on Western European 19th century coins. The FIB-FESEM technique combines focused ion beam with innovative gas etching chemistry and advanced scanning electron microscopy technologies to provide high resolution imaging down to the nano scale level. This technique can be considered micro-invasive as the Ga ions microbeam yields trenches which size is usually < 10 μm; not detectable at the macroscopic level. The trench obtained extends from the outer corrosion layers down to the metal core of the coin providing an image with high contrast between the different compositional phases and the grained microtexture of the coin. Figure 6 shows the FESEM micrographs of the trenchs obtained for the coins DF01 (a) and DF02 (c). The images acquired at higher magnification DF01 (b) and DF02 (d) show in detail the micromorphology of the outer part of the coin. In both cases, the deeper regions were composed of silver with an average yield of 1.5 wt % copper for DF01 and even up to 15 wt% copper for DF02. Remarkably, this region exhibits different rounded domains whose average size is ca. 50% larger for DF01 than for DF01. On the other hand, the external layer of the DF01 presents some porosity being accompanied by cracks and crevices until a deep of ca. 5 μm, while the corrosion layer of DF02 looks like a dense

barrier also crossed by cracks and crevices. The remarkable difference between both corrosion layers is reinforced by that existing in their chemical composition: for DF01 there is a light enrichment of copper, whose proportion increases until a 5.6 %wt, whereas in the corrosion layer of the coin DF02 the proportion of copper increases at ca. 25 %wt.

These data are in principle consistent with the differences observed in the voltammetric response of those coins, depicted in Figure 7. As can be seen in this Figure, although of similar age and composition, the voltammograms of coins DF01 and DF02 exhibit differences both in the negative-going and positive-going potential scans, thus suggesting that even subtle textural differences can produce appreciable differences in the VIMP response. Consistently with the 'modern' character of such coins, the values of the $i_p(C_{Cu})/i_p(C_{Pb})$ ratio are clearly larger than those measured for Polish coins, in agreement with the expected increase of this ratio with the corrosion time [53].

3.4. Long-term corrosion kinetics

The peculiar grouping of peak current ratios shown in Figure 5 and their variation on the copper and lead loadings of the base metal can be examined on the basis of kinetic equations for long-term corrosion. It is well-known that, under ordinary conditions, metal corrosion is 'electrochemical', constituted by anodic (metal oxidation) and cathodic (oxygen reduction) reactions occurring in different sites of the metal surface covered by a thin electrolyte layer. In the case of the studied coins, one can consider that the coins have experienced a uniform corrosion, anodic and cathodic sites being spatially separated and distributed randomly over the surface. In this situation, both the reactions of metal dissolution and oxygen reduction reaction are essentially irreversible and the metal surface has a macroscopically uniform "mixed" potential. Following the closure of Venkatraman et al. [56], the Butler–Volmer expressions for the current densities of metal oxidative dissolution and oxygen reduction, $i_{M/M^{n+}}$ and i_{O_2/OH^-} are:

$$i_{M/M^{n+}} = i^{o}_{M/M^{n+}} \exp\left(\frac{n(1-\beta_{M/M^{n+}})F}{RT} \left(E_{corr} - E^{o}_{M/M^{n+}} \right) \right) \qquad (1)$$

$$i_{O_2/OH^-} = i^{o}_{O_2/OH^-} \exp\left(-\frac{m\beta_{O_2/OH^-})F}{RT}\left(E_{corr} - E^{o}_{O_2/OH^-}\right)\right)\left(\frac{c^{O_2}_{x=0}}{c^{O_2}_{satur}}\right) \qquad (2)$$

where m denotes the electrons transferred in the rate determining step of O_2 reduction (either 2 and 4 for the 2e- and 4e-pathways), $i_{M/M^{n+}}$, i_{O_2/OH^-} are the corresponding exchange current densities, and $\beta_{M/M^{n+}}$, β_{O_2/OH^-} are the corresponding electron transfer coefficients. In this formulation, the corrosion current, given by $i_{corr} = i_{M/M^{n+}} = -i_{O_2/OH^-}$ being controlled, as a limiting cases, by the diffusion of O_2 through the electrolyte layer or the kinetics of the electron transfer processes. Subsequent modeling of the early stages of corrosion when there is a nascent porous oxide film on the metal surface with occluded electrolyte, involves consideration of the conductivity, porosity and thickness of the porous oxide layer, the contact potential difference and specific contact resistivity of the metal–oxide interface [57].

Long-term corrosion of metals, however, is in general treated using empirical equations, experimental data being fitted in general to a potential rate law [58,59]. For our purposes, the oxidation of the metal M to the metal oxide can be operationally treated using solid state reaction kinetics. Here, the advance of the reaction is represented in terms of the conversion fraction, α ($0 < \alpha < 1$), defined as the molar fraction of obtained product and assuming that at the end of the reaction the reactant is ultimately converted into the product. Much kinetic equations can be expressed as [60,61]:

$$\frac{d\alpha}{dt} = k(1-\alpha)^{\gamma} \qquad (3)$$

Then, the variation of the net amount of metal oxide by surface unit (mol cm^{-2} or g cm^{-2}), x_{Mox}, with time would be equivalent to the decrease of the corresponding amount of metal, x_M. Introducing the initial surface concentration of the metal M, c_M, results $\alpha = x_{Mox}/c_M = 1-x_M/c_M$ and the rate law can be expressed as:

$$\frac{dx_M}{dt} = -c_M k_M x_M^{-\gamma} \qquad (4)$$

Integration of the above equation yields:

$$x_{\mathrm{M}} = [c_{\mathrm{M}}^{1+\gamma} - (1+\gamma)c_{\mathrm{M}}k_{\mathrm{M}}t]^{\frac{1}{1+\gamma}} \qquad (5)$$

$$x_{\mathrm{Mox}} = c_{M} - [c_{\mathrm{M}}^{1+\gamma} - (1+\gamma)c_{\mathrm{M}}k_{\mathrm{M}}t]^{\frac{1}{1+\gamma}} \qquad (6)$$

where k_{M} is the rate constant for the solid state oxidation process. The case of copper plus lead-containing silver coins can be approximated as the corrosion of an alloy containing two oxidizable metals initially in surface concentrations c_{Cu}, c_{Pb}. Here, two extreme possibilities can be considered:

i) The metals are concentrated in different sites and form independent corrosion cells so that one can assume that they are oxidized independently at different rates. In these circumstances, the peak currents of the voltammetric peaks resulting from the reduction of the corrosion products of copper and lead, i_{p}(Cuox), i_{p}(Pbox), under fixed electrochemical conditions (electrolyte, potential scan rate, etc.) would satisfy the relationship:

$$\frac{i_{\mathrm{p}}(\mathrm{Cuox})}{i_{\mathrm{p}}(\mathrm{Pbox})} = g\frac{x_{\mathrm{Cuox}}}{x_{\mathrm{Pbox}}} = g\frac{c_{\mathrm{Cu}} - [c_{\mathrm{Cu}}^{1+\alpha} - (1+\alpha)c_{\mathrm{Cu}}k_{\mathrm{Cu}}t]^{\frac{1}{1+\alpha}}}{c_{\mathrm{Pb}} - [c_{\mathrm{Pb}}^{1+\delta} - (1+\delta)c_{\mathrm{Pb}}k_{\mathrm{Pb}}t]^{\frac{1}{1+\delta}}} \qquad (7)$$

g being an electrochemical constant which express the different intrinsic voltammetric response of the corrosion products of copper and lead. Testing the above equation, however, was made difficult by the low lead concentration in a significant fraction of the studied coins (see Table 2), thus increasing the uncertainty in those concentrations. This was reflected in a relatively high data dispersion in the representations of i_{p}(Cuox)/i_{p}(Pbox) vs. $c_{\mathrm{Cu}}/c_{\mathrm{Pb}}$, so that no conclusive results can be established.

ii) If the metals are mixed so that they are simultaneous and competitively oxidized, the corrosion rate would be:

$$i_{corr} = -i_{O_2/OH^-} = i_{Cu/Cuox} + i_{Pb/Pbox} \qquad (8)$$

This relationship can be transformed into a solid state rate law of the form:

$$\frac{d\alpha}{dt} = k_{Cu}(1-\alpha_{Cu})^{\alpha} + k_{Pb}(1-\alpha_{Pb})^{\delta} \qquad (9)$$

where α represents the fractional conversion of the reaction as measured from O_2 consumption.

In the studied case, one can approximate that all coins have experienced corrosion under similar uniform conditions during a common time. Then, Eq. (7) for the independent corrosion case (i) yields:

$$\frac{i_p(\text{Cuox})}{i_p(\text{Pbox})} = g\,\frac{c_{Cu}\{1-[c_{Cu}^{\alpha}-h_{Cu}]^{\frac{1}{1+\alpha}}\}}{c_{Pb}\{1-[c_{Pb}^{\delta}-h_{Pb}]^{\frac{1}{1+\delta}}\}} \qquad (10)$$

h_{Cu}, (= $(1+\alpha)k_{Cu}t$) h_{Pb} ((= $(1+\delta)k_{Pb}t$) being two constants depending on the corrosion time. Such constants would be representative of the extent of the corrosion and could be understood, ideally, as reflecting the degree of coverage of the respective metal surface by the corresponding corrosion product.

Solving Eq. (9) corresponding to the simultaneous oxidation case (ii) requires the disposal of a relationship between α, α_{Cu} and α_{Pb}. A single approximation can be proposed based on the assumption that, at a given corrosion time, there is a given net amount of total (copper plus lead) corrosion products and that copper corrosion can be approached by Eq. (6). The, the net amount of lead corrosion products would be simply the difference between a constant term *G* and the generated copper corrosion products so that the peak current ratio measured in voltammetric experiments would satisfy:

$$\frac{i_{\mathrm{p}}(\mathrm{Cuox})}{i_{\mathrm{p}}(\mathrm{Pbox})} = g\,\frac{c_{\mathrm{Cu}}\{1-[c_{\mathrm{Cu}}^{\alpha}-h_{\mathrm{Cu}}]^{\frac{1}{1+\alpha}}\}}{G-c_{\mathrm{Cu}}\{1-[c_{\mathrm{Cu}}^{\alpha}-h_{\mathrm{Cu}}]^{\frac{1}{1+\alpha}}\}} \qquad (11)$$

Remarkably, experimental data in Figure 5 can be satisfactorily fitted to this equation assuming that there is an essentially complete coverage of the copper by its corrosion products, using a common value (0.33±0.01) of the electrochemical coefficient, *g*, and different values of the parameter *G*. This would be characteristic of the coinage, data in Figure 5 corresponding, respectively, to *G* = 6.7, 10.6 and 20.0 in units of copper % wt.

3.5. Discussion

The above data treatment suggested that it is possible to assign a distinctive electrochemical response to the different mints as reflected in the numerical value of the (semi)empirical parameter *G*. The differences in *G* values, which would be representative of the overall extent of the corrosion, would result from the amplification during the corrosion process (in principle common for all tested coins) of the textural differences between the coins proceeding from different mints. This situation would be parallel to that illustrated in FIB-FESEM experiments in Figure 6. The DF-01 and DF02 coins, although of quite similar composition and essentially identical macroscopic appearance, displayed significant textural differences apparently resulting in drastic differences in their corrosion layers. By analogy, it would be conceivable that the differences in the voltammetric data summarized in Figure 5 reflect the mint differences of the coins and their grouping into three different mints. It is pertinent to underline that the fitting of experimental data to Eq. (11) was essentially semiempirical, the fact that such experimental data could be fitted with a unique general expression using a common value of the electrochemical coefficient *g*, denotes that there is internal consistency in the set of simplifying assumptions used in the above reasoning.

Accordingly, voltammetric data suggest that there is a reasonable possibility of dividing the studied coin samples as resulting from the use of two different metal sources in three different mints. These are summarized in Figure 8 where the studied coins are ascribed to A and B XRF groups and I to III VMP groups. Combining such ascriptions, one can propose a tentative chronological scheme considering conjointly XRF and VIMP data based on the aforementioned assumptions. This scheme can be summarized as: i) two

metal sources (A and B) and three mints (I to III) can be discerned. Mints I and III were used in all the Boleslaus plus Mieszko periods whereas mint I is represented in the studied samples only after the Boleslaus 1000-1010 period; ii) Mint II used, apparently, only metal source B, whereas mints I and III used both sources A and B; iii) metal source A was apparently not used during the Mieszko reign. This scheme would be consistent with historical data on the improvement of the monetary emission carried out during the Mieszko reign [5].

It is important to highlight that all archaeological finds prior to 1030 are concentrated in the Greater Poland (Wielkopolska) region, mainly around Poznan, Gnieezno, Kruszwica and Plock [62]. The coexistence of coins from Boleslaus and Mieszko has indicated that they were both probably minted in the same area and at approximately the same time. The maximum correlation has been observed for denarii minted by Mieszko and the PRINCES POLONIE type, minted by Boleslaus. Moreover, the archaeological evidence points towards the decentralization of mints during the studied historical period [63]. Accordingly, the differences deduced from the VIMP analysis could be associated to various minting practices related to specific geographical zones of Greater Poland.

4. Conclusions

Analysis of nanosamples from the corrosion layers of a group of 20 Polish denarii of Boleslaus the Brave and his son Mieszko II during the X–XI centuries the using the voltammetry of immobilized particles methodology provided well-defined voltammetric responses in contact with aqueous acetate buffer mainly representative of the reduction of copper and lead corrosion products.

Experimental data were consistent with the previous hypothesis [5] of the use of two different metal sources and suggested the grouping of the studied coins into three sets possibly corresponding to three different mints. This hypothesis would be consistent with semiempirical analysis of the experimental values of the ratio between the peak currents for the reduction of copper and lead corrosion products and would also be supported by complementary FIB-FESEM experiments carried out on 19^{th} century silver coins from different mints. The above results, exploiting the capabilities of the voltammetry of immobilized particles, suggest the possibility of using voltammetric

data for acquiring archaeometric information even using nanosamples from archaeological objects.

Acknowledgements: Financial support from the MINECO Projects CTQ2014-53736-C3-1-P and CTQ2014-53736-C3-2-P which are supported with ERDF funds is gratefully acknowledged. The authors are very grateful to the Polish Ministry of Science and Higher Education for partly financing the work presented in this paper through a grant within the framework of the National Program for the Development of the Humanities (Decision No. 0100/NPRH3/H12/82/2014) and also wish to thank Dr. José Luis Moya López and Mr. Manuel Planes Insausti (Microscopy Service of the Universitat Politècnica de València) for technical support.

References

[1] D.A. Scott, Metallography and Microstructure of Ancient and Historic Metals, The Getty Conservation Institute, Paul Getty Museum, Malibu (1991).

[2] G. Wojtowicz, A. Wojtowicz, Historia Monetarna Polski, Twigger, Warszawa (2003).

[3] R. Kiersnowski, Począ tki Pieniądza Polskiego, Wiedza Powszechna, Warszawa (1962).

[4] S. Suchodolski, Moneta polska w X/XI wieku, Wiadomos´ci Numizmatyczne XI (1967) 67–193.

[5] J.M. del Hoyo-Meléndez, P. Swit, M. Matosz, M. Wozniak, A. Klisinska-Topacz, L. Bratasz, Micro-XRF analysis of silver coins from medieval Poland, Nucl. Inst. Meth. Phys. Res. B 349 (2015) 6–16.

[6] H. Młodecka, P. Chabrzyk, Analiza XRF denarow Bolesława Chrobrego i jego syna Mieszka Bolesławowica w s´wietle wybranych monet z przełomu X i XI wieku – XRF analysis of denarii of Boleslaus the Brave and his son Mieszko Bolesławowic in light of selected coins from the turn of the 10th century, Biuletyn Numizmatyczny 3 (2010) 171–178.

[7] A. Buko, ‘‘Tribal’’ societies and the rise of early medieval trade: archaeological evidence from Polish territories (eight-tenth centuries), in: J. Henning (Ed.), Post-Roman Tozwns, Trade and Settlement in Europe and Byzantium: The Heirs of the Roman West, Walter de Gruyter, Berlin (2007), pp. 431–450.

[8] D. Rozmus, Srebrne zamieszanie, Ilcusiana 3 (2010) 7–16.

[9] I. Blanchard, Mining, Metallurgy and Minting in the Middle Ages, Steiner, Stuttgart (2001).

[10] A. Buko, The Archaeology of Early Medieval Poland: Discoveries, Hypotheses, Interpretations (East Central and Eastern Europe in the Middle Ages, 450–1450), Brill, Leiden (2008).

[11] G. Giovannelli, S. Natali, B. Bozzini, A. Siciliano, G. Sarcinelli, R. Vitale, Microstructural characterization of early western greek incuse coins, Archaeometry 47 (2005) 817–833.

[12] J. Corsi, F. Grazzi, A. Lo Giudice, A. Re, A. Scherillo, D. Angelici, S. Allegretti, F. Barello, Compositional and microstructural characterization of Celtic silver coins

from northern Italy using neutron diffraction analysis. Microchem. J. 126 (2016) 501–508.

[13] C. Mancini, P. Petrillo Serafin, Identification of ancient silver-plated coins by means of neutron absorption, Archaeometry, 18 (1976) 214–217.

[14] P. Budd, D. Gale, A.M. Pollard, R.G. Thomas, P.A. Williams, Evaluating lead isotope data: further observations, Archaeometry 35 (1993) 241–247.

[15] M. Ponting, J.A. Evans, V. Pashley, Fingerprints of Roman mints using laser-ablation MC-ICP-MS lead isotope analysis. Archaeometry 45 (2003) 591–597.

[16] M. Milazzo, Radiation applications in art and archaeometry X-ray fluorescence applications to archaeometry. Possibility of obtaining non-destructive quantitative analyses, Nucl. Instr. Meth. Phys. Res. B 213 (2004) 683–692.

[17] R. Linke, M. Schreiner, Energy dispersive X-ray fluorescence analysis and X-Ray microanalysis of medieval silver coins: an analytical approach for nondestructive investigation of corroded metallic artifacts, Mikrochim. Acta 133 (2000) 165–170.

[18] R. Linke, M. Schreiner, G. Demortier, The application of photon, electron and proton induced X-ray analysis for the identification and characterization of medieval silver coins, Nucl. Instr. Meth. Phys. Res. B 226 (2004) 172–178.

[19] R. Linke, M. Schreiner, G. Demortier, M. Alram, H. Winter, The provenance of medieval silver coins: analysis with EDXRF, SEM/EDX and PIXE, in: K. Janssens, R. Van Grieken (Eds.), Comprehensive Analytical Chemistry XLII, Non-Destructive Micro Analysis of Cultural Heritage Materials, Elsevier, Amsterdam, 2004, pp. 605–633.

[20] F. Rizzo, G.P. Cirrone, G. Cuttone, A. Esposito, S. Garraffo, G. Pappalardo, L. Pappalardo, F.P. Romano, S. Russo. Non-destructive determination of the silver content in Roman coins (nummi), dated to 308–311 A.D., by the combined use of PIXE-alpha, XRF and DPAA techniques. Microchem. J. 97 (2011) 286–290.

[21] F.J. Ager, B. Gómez-Tubío, A. Paúl, A. Gómez-Morón, S. Scrivano, I. Ortega-Feliu, M.A. Respaldiza, Combining XRF and GRT for the analysis of ancient silver coins. Microchem. J. 126 (2016) 149–154.

[22] J. Peris-Vicente, F.M. Valle-Algarra, M.A. Ferrer-Eres, J.V. Gimeno-Adelantado, R. Mateo-Castro, M.D. Soriano-Piñol, Archaeometrical study of paleometallurgical materials from the archaeological site “Cerro de las Balsas — Chinchorro” (La Albufereta, Alacant, Spain). Microchem. J. 90 (2008) 142–146.

[23] M.A. Ferrer-Eres, J. Peris-Vicente, F.M. Valle-Algarra, J.V. Gimeno-Adelantado, S. Sánchez-Ramos, M.D. Soriano-Piñol, Archaeopolymetallurgical study of materials from an Iberian culture site in Spain by scanning electron microscopy with X-ray microanalysis, chemometrics and image analysis. Microchem. J. 95 (2010) 298-305.
[24] T.H. Rehren, E. Pernicka, Coins, artefacts and isotopes–archaeometallurgy and archaeometry, Archaeometry 50 (2008) 232–248.
[25] R. Linke, M. Schreiner, G. Demortier, M. Alram, The determination of the provenance of medieval silver coins: potentials and limitations of X-ray analysis using photons, electrons or protons, X-Ray Spectrom. 32 (2003) 373–380.
[26] M. Carl, M.L. Young, Complementary analytical methods for analysis of Ag-plated cultural heritage objects. Microchem. J. 126 (2016) 307–315.
[27] L. Lutterotti, F. Dell'Amore, D.E. Angelucci, F. Carrer, S. Gialanella, Combined X-ray diffraction and fluorescence analysis in the cultural heritage field. Microchem. J. 126 (2016) 423–430.
[28] F. Scholz, B. Meyer, Electroanalytical Chemistry, A Series of Advances vol. 20 (1998) 1–86.
[29] F. Scholz, U. Schröder, R. Gulabowski, A. Doménech-Carbó, Electrochemistry of Immobilized Particles and Droplets, 2nd edit. Springer, Berlin-Heidelberg (2014).
[30] A. Doménech-Carbó, M.T. Doménech-Carbó, V. Costa, Electrochemical Methods in Archaeometry, Conservation and Restoration. Monographs in Electrochemistry Series, F. Scholz, Ed. Springer, Berlin-Heidelberg (2009).
[31] A. Doménech-Carbó, J. Solid State Electrochem. 14 (2010) 363–379.
[32] V. Costa, K. Leyssens, A. Adriaens, N. Richard, F. Scholz, Electrochemistry reveals archaeological materials, J. Solid State Electrochem. 14 (2010) 449–451.
[33] F. Arjmand, A. Adriaens, Electrochemical quantification of copper-based alloys using voltammetry of microparticles: optimization of the experimental conditions, J. Solid State Electrochem. 16 (2012) 535–543.
[34] N. Souissi, L. Bousselmi, S. Khosrof, E. Triki, Voltammetric behaviour of an archeaological bronze alloy in aqueous chloride media, Materials and Corrosion 55 (2004) 284–292.
[35] M. Serghini-Idrissi, M.C. Bernard, F.Z. Harrif, S. Joiret, K. Rahmouni, A. Srhiri, H. Takenouti, V. Vivier, M. Ziani, Electrochemical and spectroscopic characterizations of patinas formed on an archaeological bronze coin, Electrochimica Acta 50 (2005) 4699–4709.

[36] A. Doménech-Carbó, M.T. Doménech-Carbó, I. Martínez-Lázaro, Electrochemical identification of bronze corrosion products in archaeological artefacts. A case study, Microchim. Acta 162 (2008) 351–359.

[37] D. Satovic, S. Martinez, A. Bobrowski, Electrochemical identification of corrosion products on historical and archaeological bronzes using the voltammetry of micro-particles attached to a carbon paste electrode, Talanta 81 (2010) 1760–1765.

[38] A. Doménech-Carbó, M.T. Doménech-Carbó, I. Martínez-Lázaro, Layer-by-layer identification of copper alteration products in metallic works of art using the voltammetry of microparticles approach, Analytica Chimica Acta 610 (2010) 1–9.

[39] A. Doménech-Carbó, M.T. Doménech-Carbó, M.A. Peiró-Ronda, 'One-touch' voltammetry of microparticles for the identification of corrosion products in archaeological lead, Electroanalysis 23 (2011) 1391−1400.

[40] D. Blum, W. Leyffer, R. Holze, Pencil-Leads as New Electrodes for Abrasive Stripping Voltammetry, Electroanalysis 8 (1996) 296–297.

[41] V. Costa, F. Urban, Lead and its alloys: metallurgy, deterioration and conservation, Reviews in Conservation, International Institute of Conservation 6 (2005) 38–48.

[42] A. Doménech-Carbó, M.T. Doménech-Carbó, M.A. Peiró-Ronda, L. Osete-Cortina, Authentication of archaeological lead artifacts using voltammetry of microparticles: the case of the *Tossal de Sant Miquel* Iberian plate, Archaeometry 53 (2011) 1193–1211.

[43] A. Doménech-Carbó, Tracing, authentifying and dating archaeological metal using the voltammetry of microparticles, Anal. Methods 3 (2011) 2181–2188.

[44] A. Doménech-Carbó, M.T. Doménech-Carbó, M.A. Peiró-Ronda, Dating archaeological lead artifacts from measurement of the corrosion content using the voltammetry of microparticles, Anal. Chem. 83 (2011) 5639–5644.

[45] A. Doménech-Carbó, M.T. Doménech-Carbó, S. Capelo, T. Pasíes, I. Martínez-Lázaro, Dating archaeological copper/bronze artifacts using the voltammetry of microparticles, Angew. Chem. Int. Ed. 53 (2014) 9262–9266.

[46] S. Capelo, P.M. Homem, J. Cavalheiro, I.T.E. Fonseca, Linear sweep voltammetry: a cheap and powerful technique for the identification of the silver tarnish layer constituent, J. Solid State Electrochem. 17 (2013) 223–234.

[47] G. Cepriá, O. Abadías, J. Pérez-Arantegui, J.R. Castillo, Electrochemical behavior of silver-copper alloys in voltammetry of microparticles: a simple method for screening purposes, Electroanalysis, 13 (2001) 477–483.

[48] A. Doménech-Carbó, M.T. Doménech-Carbó, T. Pasíes, M.C. Bouzas, Modeling corrosion of archaeological silver-copper coins using the voltammetry of immobilized particles, Electroanalysis 24 (2012) 1945–1955.

[49] A. Doménech-Carbó, M.T. Doménech-Carbó, T. Pasíes, M.C. Bouzas, Application of modified Tafel analysis to the identification of corrosion products on archaeological metals using voltammetry of microparticles, Electroanalysis 23 (2011) 2803–2812.

[50] N. Zakharchuk, S. Meyer, B. Lange, F. Scholz, A Comparative Study of Lead Oxide Modified Graphite Paste Electrodes and Solid Graphite Electrodes with Mechanically Immobilized Lead Oxides, Croat. Chem. Acta 73 (2000) 667–704.

[51] S. Komorsky-Lovric, M. Lovric, A.M. Bond, Comparison of the square-wave stripping voltammetry of lead and mercury following their electrochemical or abrasive deposition onto a paraffin impregnated graphite electrode, Anal. Chim. Acta. 258 (1992) 299–305.

[52] M. De Keersmaecker, M. Dowsett, R. Grayburn, D. Banerjee, A. Adriaens, In-situ spectroelectrochemical characterization of the electrochemical growth and breakdown of a lead dodecanoate coating on a lead substrate, Talanta. 132 (2015) 760–768.

[53] A. Doménech-Carbó, M.T. Doménech-Carbó, J. Redondo-Marugán, L. Osete-Cortina, M.V. Vivancos-Ramón, Electrochemical characterization of corrosion products in leaded bronze sculptures considering ohmic drop effects on Tafel analysis, Electroanalysis 28 (2016) 833–845.

[54] G.M. Ingo, E. Angelini, T. de Caro, G. Bultrini, Combined use of surface and micro-analytical techniques for the study of ancient coins. Appl. Phys. A 79 (2004) 171–176.

[55] I. Uzonyi, R. Bugoi, A. Sasianu, Á.Z. Kiss, B. Constantinescu, M. Torbágyi, Characterization of Dyrrhachium silver coins by micro-PIXE method. Nucl. Instr. Meth. Phys. Res. B 161–163 (2000) 748–752.

[56] M.S. Venkatraman, I.S. Cole, B. Emmanuel, Model for corrosion of metals covered with thin electrolyte layers: Pseudo-steady state diffusion of oxygen. Electrochim. Acta 56 (2011) 7171–7179.

[57] M.S. Venkatraman, I.S. Cole, B. Emmanuel Corrosion under a porous layer: A

porous electrode model and its implications for self-repair. Electrochim. Acta 56 (2011) 8192–8203.

[58] J.W. Spence, F.H. Haynie, F.W. Lipfert, S.D. Cramer, L.G. McDonald, Atmospheric corrosion model for galvanized steel structures, Corrosion 48 (1992) 1009–1019.

[59] S. Feliu, M. Morcillo, S. Feliu Jr.,The prediction of atmospheric corrosion from meteorological and pollution parameters—II. Long-term forecasts, Corros. Sci. 34 (1993) 415–422.

[60] H. Schmalzried, Chemical kinetics of solids. VCH Wenheim (1995).

[61] S.E. Dann, Reactions and characterization of solids. The Royal Society of Chemistry, Cambridge (2000).

[62] S. Suchodolski, Spór o początki mennictwa w Czechach i w Polsce, Wiadomości Numizmatyczne XLII (1998) 5–20.

[63] M. Rolski, Początki polityki pieniężnej na ziemiach polskich, Studia Ekonomiczne 176 (2014) 122–132.

Table 1. Characteristics of the reference alloys.

Reference	wt%Ag	wt%Cu	wt%Pb
STD1	65	35	
STD2	85	15	
STD3	94	4	2
STD4	96	4	
STD5	96	3	1
STD6	96	1	3

Table 2. Description of coin samples in this study and composition of major metal components determined by XRF [5].

Coin	King	Period	wt%Ag	wt%Cu	wt%Pb
806	B	995-1005	89	9.2	0.8
812	B	995-1005	91.2	6.9	0.9
809	B	995-1005	94.1	4.3	0.6
770	B	1000-1010	94.5	2.5	2
800	B	1000-1010	94.6	3.5	0.9
779	B	after 1010	94.7	3.1	1.2
782	B	after 1010	94.3	4.7	0.5
783	B	after 1010	96.8	2.3	0.5
788	B	after 1010	94.6	3.7	0.7
791	B	after 1010	94.9	4.1	0.5
793	B	after 1010	90.3	7.6	1.1
795	B	after 1010	88.4	10	0.6
796	B	after 1010	94.6	4	0.5
797	B	after 1010	94.1	4.3	0.6
21282	M	1010-1020	93.9	4.5	0.6
753	M	1010-1020	93.1	5.3	0.5
762	M	1010-1020	94.9	3.4	0.6
764	M	1010-1020	96.1	2.5	0.5
765	M	1010-1020	93.9	4.6	0.5
766	M	1010-1020	94.3	4	0.7

Figures

Figure 1. SWVs of samples from coins a,b) 766 and c,d) 783 attached to graphite electrodes immersed into 0.25 M sodium acetate buffer, pH 4.75. a,b) voltammograms at sample modified electrodes (black lines) and at the bare graphite electrode in the same electrolyte (red lines); c,d) voltammetric curves after subtracting the corresponding background current. Potential scan initiated at: a) +1.25 V in the negative direction and b) −1.05 V in the positive direction. Potential step increment 4 mV; square wave amplitude 25 mV; frequency 5 Hz.

Figure 2. Region between +0.40 and −0.10 V of SWVs of: a) reference material containing 96%wt Ag plus 4%wt Cu, b-d) samples from coins b) 800; c) 796; d) 762 attached to graphite electrodes immersed into 0.25 M sodium acetate buffer, pH 4.75. Potential scan initiated at: a) +1.25 V in the negative direction and b) −1.05 V in the positive direction. Potential step increment 4 mV; square wave amplitude 25 mV; frequency 5 Hz.

Figure 3. Region between +0.80 and −0.40 V of SWVs of samples from coins a) 793; b) 795; c)782; d) 791; e) 753; f) 788 attached to graphite electrodes immersed into 0.25 M sodium acetate buffer, pH 4.75. Potential scan initiated at −1.05 V in the positive direction. Potential step increment 4 mV; square wave amplitude 25 mV; frequency 5 Hz. Inset: Photograph of coin 762.

Figure 4. Variation of the percentage of a) Cu and b) Pb on the percentage of Ag, determined from XRF data, for the studied coins. From data in ref. [5].

Figure 5. Plots of $i_p(C_{Cu})/i_p(C_{Pb})$ vs. the percentage of Cu for coin samples in this study. Data from VIMP experiments such as in Figure 1a. Squares: Boleslaus 995-1005; solid squares: Boleslaus 1000-1010; triangles: Boleslaus after 1010 and solid triangles: Mieszko 1010-1020. Lines correspond to theory using Eq. (11) taking g = 0.33 and G = 6.7, 10.6 and 20.0, respectively.

Figure 6. FIB-FESEM images of trench *ca.* 10μm length and *ca.* 15μm depth generated

by FIB in the region of interest in the coins a,b) DF01 and c,d) DF02 at two different magnifications.

Figure 7. SWVs of samples from coins a,b) DF02 and c,d) DF01 attached to graphite electrodes immersed into 0.25 M sodium acetate buffer, pH 4.75. Potential scan initiated at: a) +1.25 V in the negative direction and b) –1.05 V in the positive direction. Potential step increment 4 mV; square wave amplitude 25 mV; frequency 5 Hz. Insets: Images of coins DF02 and DF01.

Figure 8. Tentative chronological scheme illustrating the grouping of the studied coins into three mints using two metal sources.

Figure 1.

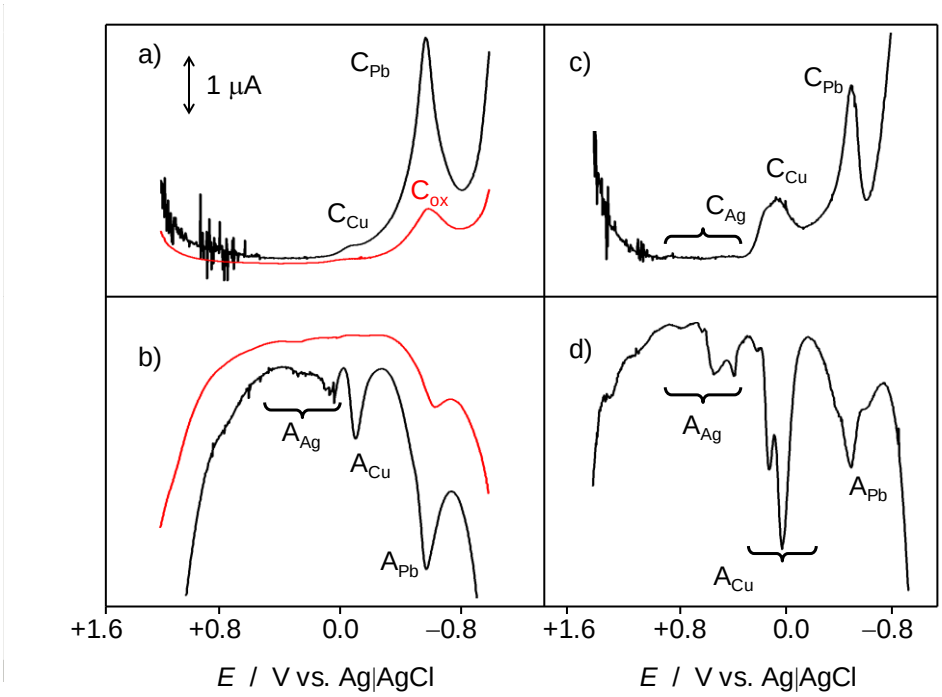
a)
1 μA
C_{Pb}
C_{Cu}
C_{ox}
c)
C_{Pb}
C_{Cu}
C_{Ag}
b)
A_{Ag}
A_{Cu}
A_{Pb}
d)
A_{Ag}
A_{Pb}
A_{Cu}
+1.6
+0.8
0.0
–0.8
+1.6
+0.8
0.0
–0.8
E / V vs. Ag|AgCl
E / V vs. Ag|AgCl

Figure 2.

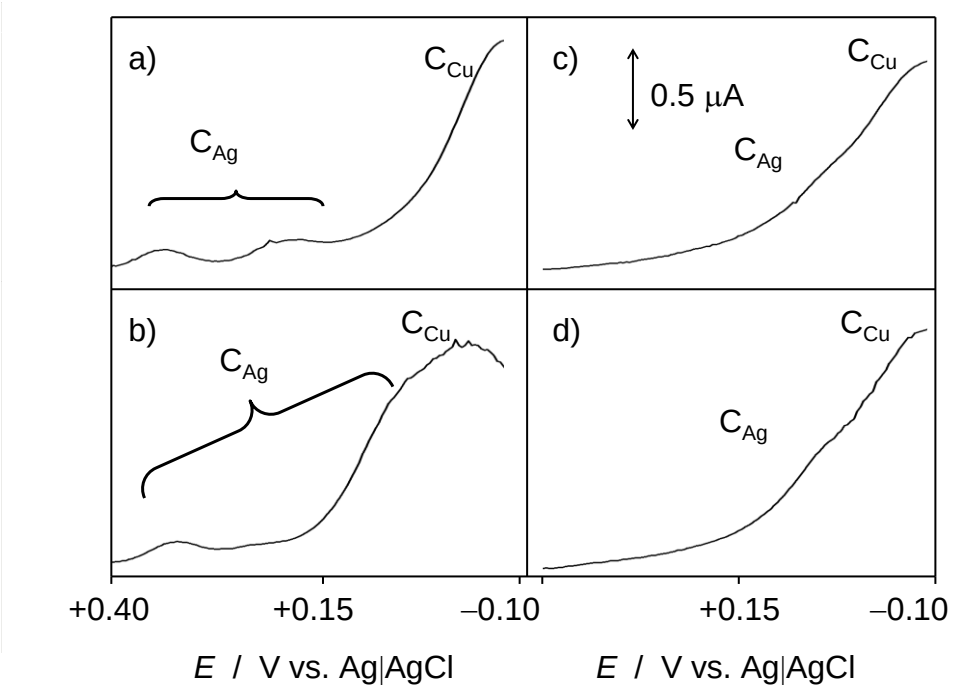
a)
C_{Cu}
C_{Ag}
c)
0.5 μA
C_{Cu}
C_{Ag}
b)
C_{Cu}
C_{Ag}
d)
C_{Cu}
C_{Ag}
+0.40
+0.15
–0.10
+0.15
–0.10
E / V vs. Ag|AgCl
E / V vs. Ag|AgCl

Figure 3.

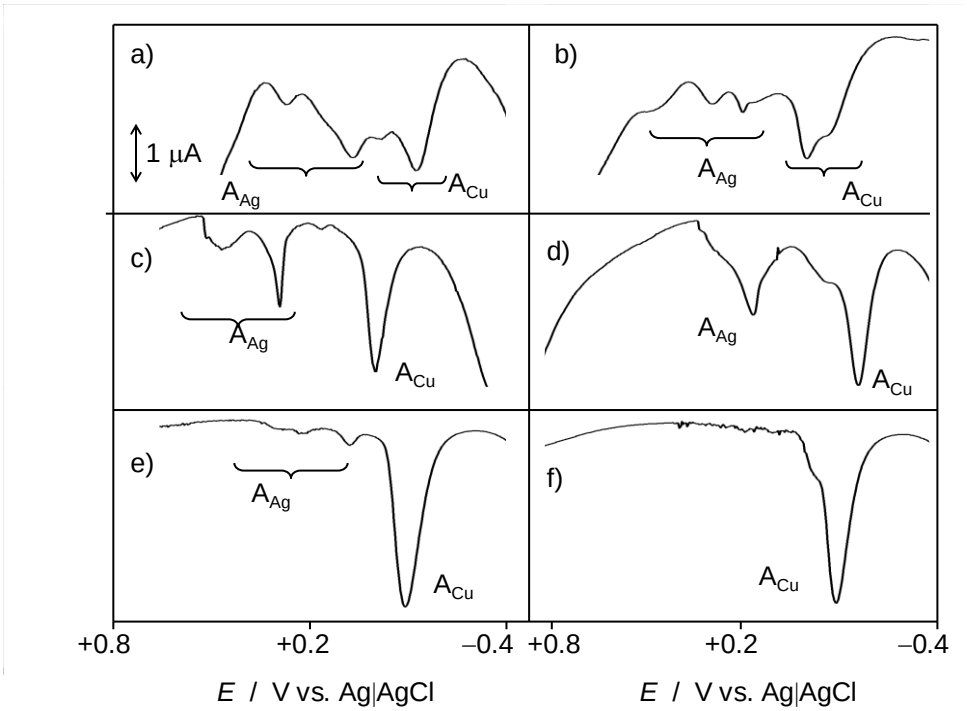
a)
1 μA
A_{Ag}
A_{Cu}
b)
A_{Ag}
A_{Cu}
c)
A_{Ag}
A_{Cu}
d)
A_{Ag}
A_{Cu}
e)
A_{Ag}
A_{Cu}
f)
A_{Cu}
+0.8
+0.2
–0.4
+0.8
+0.2
–0.4
E / V vs. Ag|AgCl
E / V vs. Ag|AgCl

Figure 4.

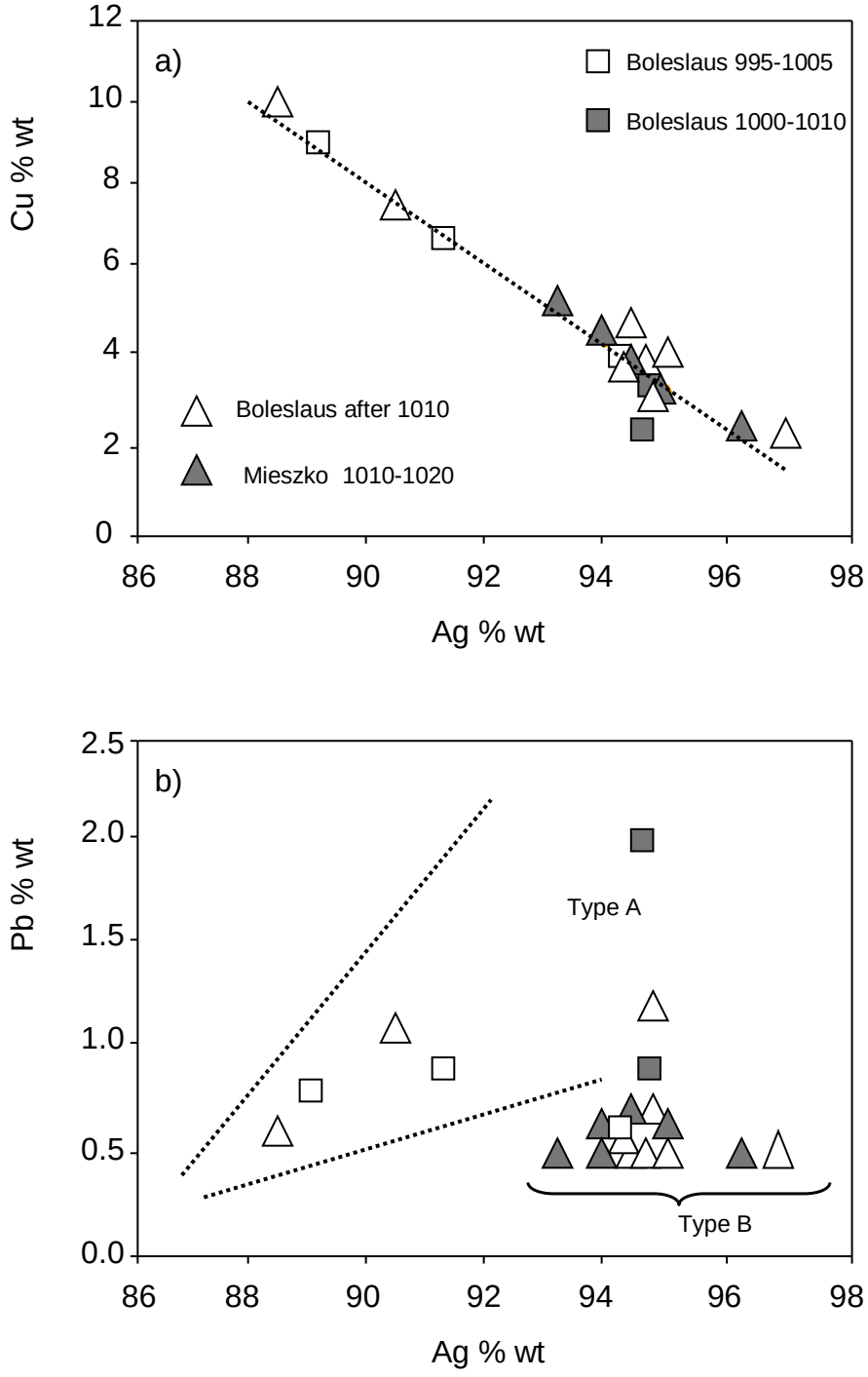
a)
Boleslaus 995-1005
Boleslaus 1000-1010
Boleslaus after 1010
Mieszko 1010-1020
Cu % wt
Ag % wt
0
2
4
6
8
10
12
86
88
90
92
94
96
98
b)
Type A
Type B
Pb % wt
Ag % wt
0.0
0.5
1.0
1.5
2.0
2.5

Figure 5.

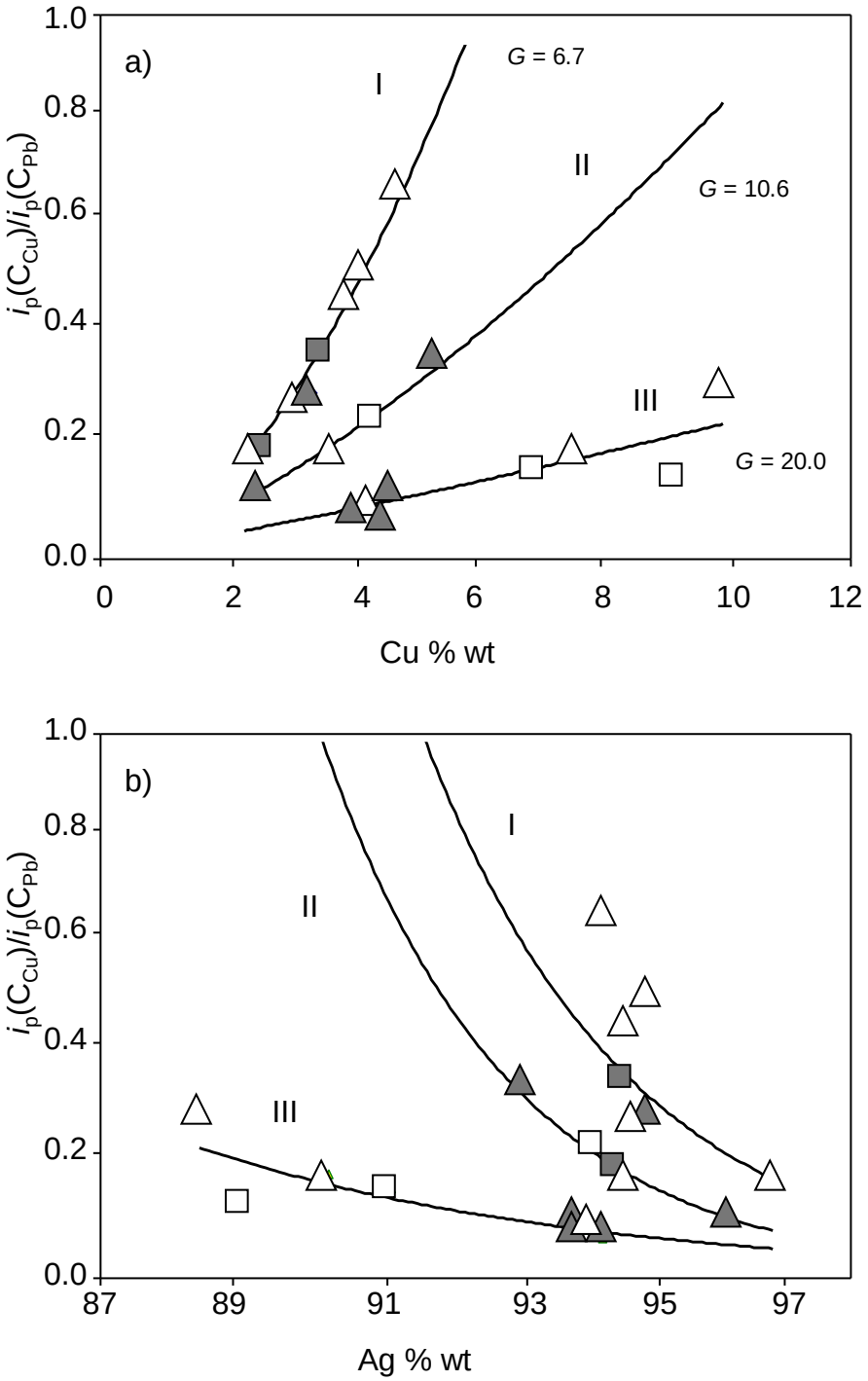
a)
G = 6.7
G = 10.6
G = 20.0
I
II
III
$i_p(C_{Cu})/i_p(C_{Pb})$
Cu % wt
b)
I
II
III
$i_p(C_{Cu})/i_p(C_{Pb})$
Ag % wt

Figure 6.

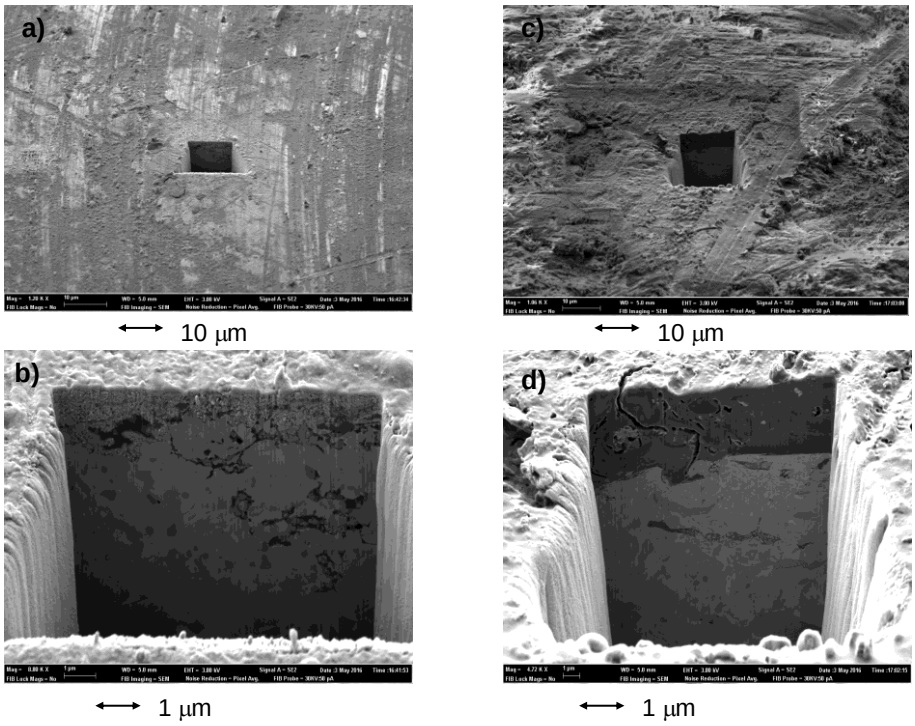

Figure 7.

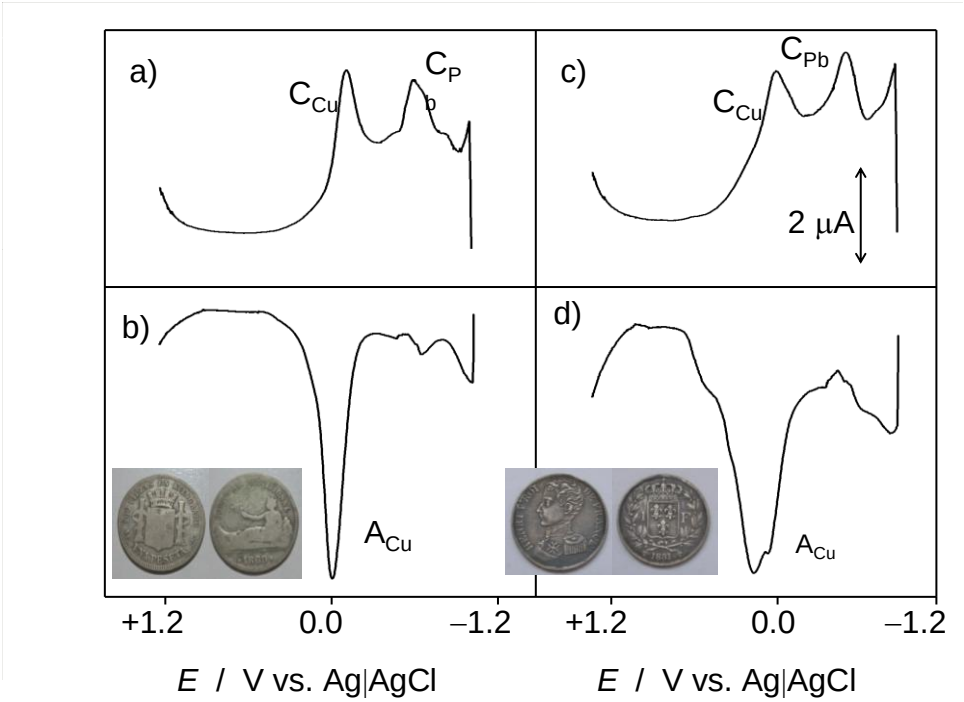
a)
C_{Cu}
C_{Pb}
c)
C_{Pb}
C_{Cu}
2 µA
b)
A_{Cu}
d)
A_{Cu}
+1.2
0.0
–1.2
+1.2
0.0
–1.2
E / V vs. Ag|AgCl
E / V vs. Ag|AgCl

Figure 8.

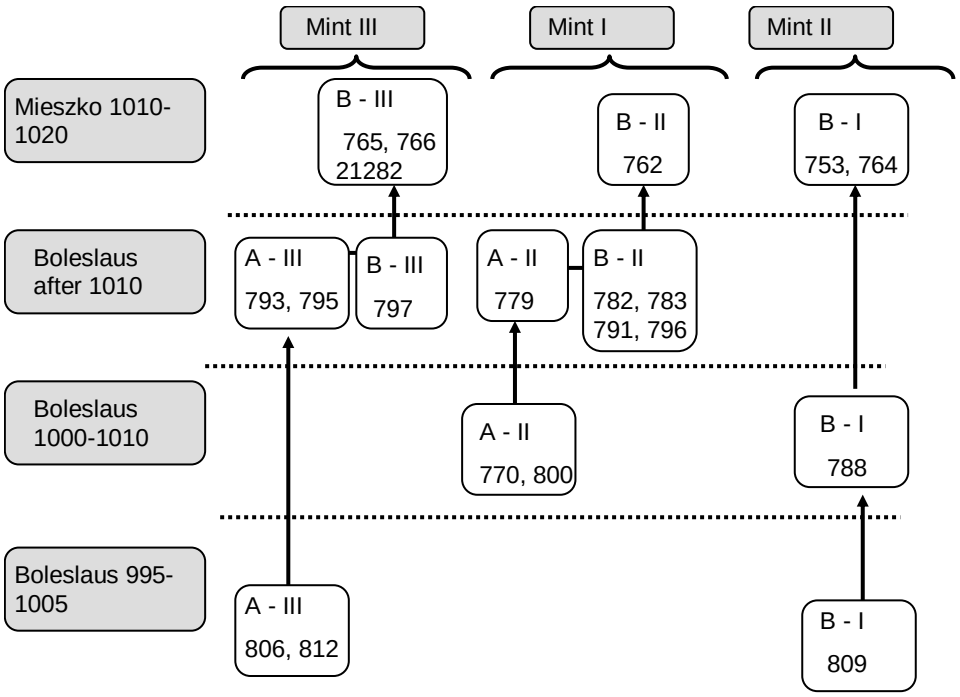
Mint III
Mint I
Mint II
Mieszko 1010-1020
B - III
765, 766
21282
B - II
762
B - I
753, 764
Boleslaus after 1010
A - III
793, 795
B - III
797
A - II
779
B - II
782, 783
791, 796
Boleslaus 1000-1010
A - II
770, 800
B - I
788
Boleslaus 995-1005
A - III
806, 812
B - I
809